Tensor temperature and shock-wave stability in a strong two-dimensional shock wave

Wm. G. Hoover and Carol G. Hoover
Ruby Valley Research Institute, Highway Contract 60, Box 598, Ruby Valley, Nevada 89833, USA
(Received 12 May 2009; published 23 July 2009)

The anisotropy of temperature is studied here in a strong two-dimensional shock wave, simulated with conventional molecular dynamics. Several forms of the kinetic temperature are considered, corresponding to different choices for the local instantaneous stream velocity. A local particle-based definition omitting any "self"-contribution to the stream velocity gives the best results. The configurational temperature is not useful for this shock-wave problem. The configurational temperature is subject to a shear instability and can give local negative temperatures in the vicinity of the shock front. The decay of sinusoidal shock-front perturbations shows that strong two-dimensional planar shock waves are stable to such perturbations.

DOI: 10.1103/PhysRevE.80.011128 PACS number(s): 02.70.Ns, 45.10.−b, 46.15.−x, 47.11.Mn

I. INTRODUCTION

Shockwaves are useful tools for the understanding of material behavior far from equilibrium [1–4]. The high-pressure physicist Percy Bridgman played a key role in the adaptation of experimental shock-wave physics to the thermodynamic characterization of materials at high pressure [4]. Because shock waves join two purely equilibrium states, shown to the left and the right of the central shock wave in Fig. 1, the experimental and the computational difficulties associated with imposing nonequilibrium boundary conditions are absent.

Begin by assuming that the flow is both stationary and one dimensional. Such a flow gives conservation of the mass, the momentum, and the energy fluxes throughout the shock wave. Thus the fluxes of mass, momentum, and energy,

$$\rho u, \quad P_{xx} + \rho u^2, \quad \rho u[e + (P_{xx}/\rho) + (u^2/2)] + Q_x,$$

are constant throughout the system, even in the far-from-equilibrium states within the shock wave. Here u is the flow velocity, the velocity in the x direction, the direction of propagation. We use conventional notation here, ρ for the density, P for the pressure tensor, e for the internal energy per unit mass, and Q_x for the component of heat flux in the shock direction, x. It is important to recognize that both the pressure tensor and the heat flux vector are measured in a local coordinate frame moving with the local fluid velocity $u(x)$.

In a different "comoving frame," this time moving with the shock velocity and centered on the shock wave, cold material enters from the left, with speed u_s (the "shock speed"), and hot material exits at the right, with speed $u_s - u_p$, where u_p is the "piston speed." Computer simulations of shock waves, using molecular dynamics, have a history of more than 50 years, dating back to the development of fast computers [5–11]. Increasingly sophisticated high-pressure shock-wave experiments have been carried out since the second world war [12].

In laboratory experiments it is convenient to measure the two speeds, u_s and u_p. These two values, together with the initial "cold" values of the density, the pressure, and the energy, make it possible to solve the three conservation equations for the "hot values" of ρ, P_{xx}, and e. A linear relation between $P_{xx}(x)$ and $V(x) = 1/\rho$, results when the mass flux $M \equiv \rho u$ is substituted into the equation for momentum conservation

$$P_{xx}(x) + M^2/\rho(x) = P_{\rm hot} + (M^2/\rho_{\rm hot}) = P_{\rm cold} + (M^2/\rho_{\rm cold}).$$

This nonequilibrium pressure-tensor relation is called the "Rayleigh line." The energy conservation relation,

$$\Delta e = -(1/2)[P_{\rm hot} + P_{\rm cold}]\Delta V,$$

based on equating the work of compression to the gain in internal energy, is called the "shock Hugoniot relation" (see Fig. 2 for both). A recent comprehensive review of shock-wave physics can be found in Ref. [3].

Laboratory experiments based on this approach have detailed the equations of state for many materials. Pressures in excess of 6 TPa (60 Mbar) have been characterized [12]. If a constitutive relation is assumed for the nonequilibrium anisotropic parts of the pressure tensor and the heat flux, the conservation relations give ordinary differential equations for the shock-wave profiles. With Newtonian viscosity and Fourier heat conduction, the resulting "Navier-Stokes" profiles have shock widths on the order of the mean-free path [7,8].

Early theoretical analyses of shock waves emphasized solutions of the Boltzmann equation. Mott-Smith's approximate solution of that equation [13], based on the weighted average of two equilibrium Maxwellian distributions, one hot and one cold, revealed a temperature maximum (and a corresponding entropy maximum) at the shock center, for shocks with a Mach number exceeding 2. The Mach number is the ratio of the shock speed to the sound speed. Twenty years later, molecular-dynamics simulations showed shock widths of just a few atomic diameters [5–8]. These narrow shock waves agreed nicely with the predictions of the

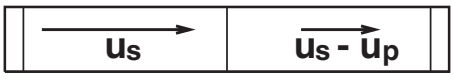

FIG. 1. A stationary one-dimensional shock wave. Cold material enters at the left with a speed u_s, passes through the shock front which separates the cold material from the hot, and exits at the right with speed $u_s - u_p$. The cold-to-hot conversion process is irreversible and corresponds to an overall entropy increase.

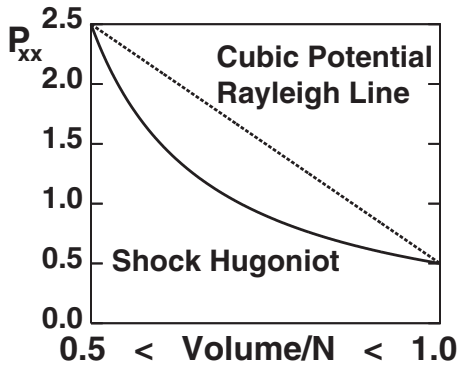

FIG. 2. Calculated Rayleigh line and shock Hugoniot relation for the simple repulsive van der Waals equation described in the text. The Rayleigh line includes nonequilibrium states within the shock while the shock Hugoniot line is the locus of all equilibrium states accessible by shocking the initial state.

Navier-Stokes equations for relatively weak shocks. At higher pressures there is a tendency for the Navier-Stokes profiles to underestimate the shock width. Some of the computer simulations have shown the temperature maximum at the shock front predicted by Mott-Smith [8,10]. These temperature maxima are constitutive embarrassments—they imply a negative heat conductivity for a part of the shock-wave profile.

Our interest here is twofold. We want to check on the stability of planar shock waves (the foregoing analysis assumes this stability) and we also want to characterize the anisotropy of temperature in the shock. This latter topic is particularly interesting now in view of the several definitions of temperature applied to molecular-dynamics simulations [8,9,14–18]. A configurational-temperature definition as well as several kinetic-temperature definitions can all be applied to the shock-wave problem.

The plan of the present work is as follows. Section II describes the material model and the computational setup of the simulations along with the computation of the shock profiles and the analysis confirming their stability. Section III also compares the various kinetic- and configurational-temperature definitions for a strong stable shock wave. Section IV details our conclusions.

II. SHOCK-WAVE SIMULATION FOR A SIMPLE MODEL SYSTEM

We simulate the geometry of Fig. 1 by introducing equally spaced columns of cold particles from a square lattice. The initial lattice moves to the right at speed u_s. The interior of the system is purely Newtonian, without any boundary, constraint, or driving forces. Those particles coming within the range of the forces ($\sigma=1$) of the right-hand boundary have their velocities set equal to u_s-u_p (the mean exit velocity) and are discarded once they reach the boundary. This boundary condition, because it corresponds to a diffusive heat sink at the exit, only affects the flow in the vicinity of that boundary. We initially chose the speeds $u_s=2$ and $u_p=1$ to correspond to twofold compression. The approximate thermal and mechanical equations of state,

$$e=(\rho/2)+T, \quad P=\rho e,$$

together with the initial values,

$$\rho_{\rm cold}=1, \quad T_{\rm cold}=0, \quad P_{\rm cold}=(1/2), \quad e_{\rm cold}=(1/2),$$

give the corresponding hot values. These two sets of thermodynamic data mutually satisfy the Rayleigh line and the shock Hugoniot relation for twofold compression from the cold state,

$$\rho_{\rm hot}=2, \quad T_{\rm hot}=(1/4), \quad P_{\rm hot}=(5/2), \quad e_{\rm hot}=(5/4).$$

The mass, the momentum, and the energy fluxes are 2, (9/2), and 6, respectively. For reasons explained below, it was necessary to modify these conditions slightly, using instead $u_s=2u_p=1.75$.

We considered a wide variety of system lengths and widths and found no significant difference in the nature of the results. For convenience we show here results for a system of length $L_x=200$ and width $L_y=40$. Because the density increases by a factor of 2 in the center of the system, the number of particles used in this case is about 12 000. The number varies during the simulation as new particles enter and old ones are discarded. The total length of the run is one shock traversal time, $200/u_s$, although the shock is itself localized near the center of the system and in fact moves very little in our chosen coordinate frame. In retrospect, the simulations could just as well have been carried out with a much smaller L_x. Because we wished to study stability, we felt it is necessary to use a relatively wide system.

For a two-dimensional classical model with a weak van der Waals repulsion, the equation of state described above follows from the simple canonical partition function:

$$Z^{1/N} \propto VTe^{-\rho/2T}, \quad PV/NkT=[\partial \ln Z/\partial \ln V]_T,$$

$$E/NkT=[\partial \ln Z/\partial \ln T]_V.$$

Our original intent was to use the smooth repulsive pair potential [19]

$$\phi=(10/\pi\sigma^2)[1-(r/\sigma)]^3 \quad \text{for} \quad r<\sigma$$

$$\rightarrow \langle \Phi \rangle \simeq (N\rho/2)\int_V \phi(r) 2\pi r dr = N\rho/2.$$

For a sufficiently large σ (3 or so) that simple equation of state was accurate. But for large σ the shock width is also so large that detailed studies are impractical. In the end we chose to set the range of the forces equal to unity, so that the initial pressure is actually zero rather than 1/2. Nevertheless, the choice of $u_s=2$ is still roughly compatible with twofold compression. Equilibrium molecular-dynamics simulations for $\sigma=1$ give the following solution to the conservation relations for twofold compression, from $\rho_0=1$ to $\rho=2$ with $u_s=2u_p=1.75$:

$$\rho u: 1.0 \times 1.75 = 2.0 \times 0.875 = 1.75,$$

$$P+\rho u^2: 0.0+1.0 \times 1.75^2 = 1.531 + 2.0 \times 0.875^2 = 3.062,$$

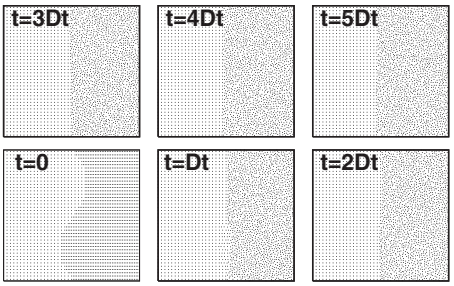

FIG. 3. Particle positions in the initial condition correspond to $t=0$. Those to the left of the sine-wave boundary move to the right at speed $u_s=1.75$ while those to the right travel at speed $u_s-u_p=u_s/2$. Particle positions at five later equally spaced times are shown too. The time interval $Dt=40/u_s$ is 2000 time steps. The 40×40 windows shown here would contain 1600 cold or 3200 hot particles at the cold and the hot densities of 1.0 and 2.0.

$$\rho u[e+(P/\rho)+(u^2/2)] = 1.75[0.0+0.0+1.531]$$
$$= 1.75[0.383+0.766+0.383]$$
$$= 1.75\times 1.531.$$

We introduced a sinusoidal perturbation in the initial conditions by using twice as many columns of particles (per unit length) to the right of a line near the center of the system,

$$x_{\text{shock}} = 6\,\sin(2\pi y/L_y).$$

The time development of a system starting with this sine-wave displacement perturbation is shown in Fig. 3. The panel corresponding to the time $t=Dt$ shows that the decay is underdamped, while the following panels show that the planar shock wave is stable.

Figure 4 illustrates the effect of the gradual underdamped flattening of the sine-wave perturbation on the density profile. The propagation of the wave is followed through five shock traversal times of the observation window used in Fig. 3.

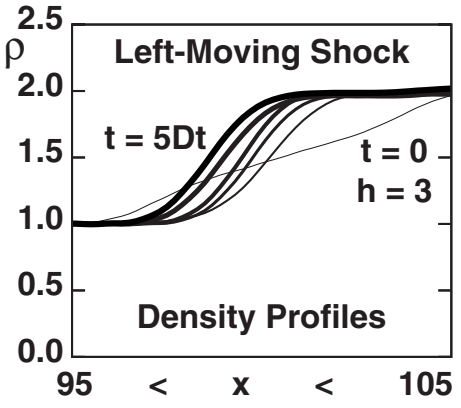

FIG. 4. Density profiles at the same times as those illustrated in Fig. 3. These one-dimensional density profiles were computed with Lucy's one-dimensional smooth-particle weight function using $h=3$ and the particle coordinates shown in Fig. 3. Increasing time corresponds to increasing line thickness as the shock wave moves slowly to the left.

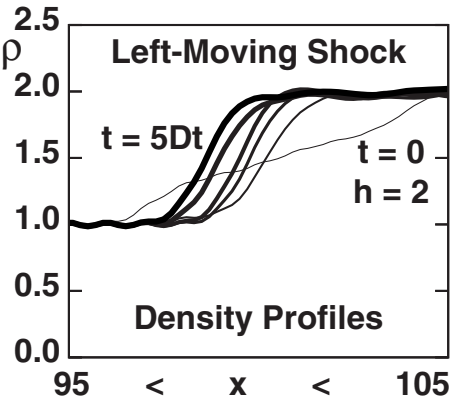

FIG. 5. Density profiles exactly as in Fig. 4, but with a reduced range, $h=2$. The shock wave moves slowly to the *left*. Note the wiggly structure, a consequence of choosing h too small.

The density profiles are computed with Lucy's one-dimensional weighting function [20,21]

$$w^{1D}(r<h) = (5/4h)[1-6(r/h)^2+8(r/h)^3-3(r/h)^4],$$

$$r<h=3,$$

$$\rightarrow \int_{-h}^{+h} w(r)dr \equiv 1.$$

The density is computed by evaluating the expression

$$\rho(x_k) = \sum w_{ik}^{1D}/L_y, \quad w_{ik}^{1D} \equiv w^{1D}(|x_i - x_k|),$$

for all combinations of particle i and grid point k separated by no more than $h=3$. For comparison density profiles using a shorter range, $h=2$, are shown in Fig. 5. These latter profiles exhibit a wiggly structure indicating a deterioration of the averaging process.

Similar conclusions, using similar techniques, have been drawn by Hardy and his co-workers [9,11], who were evidently unaware of Lucy and Monaghan's work. In their interesting analysis of a two-dimensional shock wave, Root *et al.* used a weight function like Lucy's, but with square (rather than circular) symmetry and with only a single vanishing derivative at its maximum range [11]. They discussed the ambiguities of determining temperature away from equilibrium and rightly concluded that the range of the spatial weight function needs careful consideration. Hardy [9] recently told us that his use of a spatial weighting function was motivated by a conversation with Choquard.

The profiles we show in Fig. 4 are typical and show that the shock width rapidly attains a value of about three particle diameters and has no further tendency to change as time goes on. A detailed study shows that the sine-wave amplitude exhibits underdamped oscillations on its way to planarity. Evidently, for this two-dimensional problem, the one-dimensional shock-wave structure is stable. In the next section we consider the temperature profiles for the stationary shock wave.

III. CONFIGURATIONAL AND KINETIC TEMPERATURES IN THE SHOCKWAVE

The kinetic and the configurational contributions to temperature and pressure have been discussed and explored in a variety of nonequilibrium contexts. Shockwaves, with stationary boundary conditions far from the shock front, allow the anisotropy of the kinetic temperature to be explored, analyzed, and characterized with purely Newtonian molecular dynamics. Kinetic-theory temperature is based on the notion of an equilibrium ideal gas thermometer [22–24]. The temperature(s) measured by such a thermometer is given by the second moments of the velocity distribution,

$$\{kT_{xx}^K, kT_{yy}^K\} = m\{\langle v_x^2\rangle, \langle v_y^2\rangle\},$$

where the velocities are measured in the comoving frame, with the frame moving at the mean velocity of the fluid.

A dilute Maxwell-Boltzmann gas of small hard parallel cubes undergoing impulsive collisions with a large test particle provides an explicit model tensor thermometer for the test-particle kinetic temperature [24]. The main difficulty associated with the kinetic temperature lies in estimating the mean stream velocity, with respect to which thermal fluctuations define the kinetic temperature. In what follows we compare several such definitions, in an effort to identify the best approach.

The configurational temperature is more complicated and lacks a definite microscopic mechanical model of a thermometer able to measure it. The configurational temperature is based on linking two canonical-ensemble equilibrium averages, as was written down by Landau and Lifshitz more than 50 years ago [25],

$$\{kT_{xx}^\Phi, kT_{yy}^\Phi\} = \{\langle F_x^2\rangle/\langle \nabla_x^2 \mathcal{H}\rangle, \langle F_y^2\rangle/\langle \nabla_y^2 \mathcal{H}\rangle\}.$$

Here, $\mathcal{H}$ is the Hamiltonian governing particle motion. Unlike the kinetic temperature, this configurational definition is independent of stream velocity. Its apparent dependence on rotation [19] is negligibly small for the (irrotational) shock-wave problems considered here. We apply both the kinetic and the configurational approaches to temperature measurement here, considering individual degrees of freedom within a nominally one-dimensional shock wave in two-dimensional plane geometry.

Although the notion of the configurational temperature can be defended at equilibrium, the shock-wave problem indicates a serious deficiency in the concept. An isolated row or column of particles, all with the same y or x coordinate and interacting with repulsive forces is clearly unstable to transverse perturbations. The symptom of this instability is a negative "force constant"

$$(\langle \nabla\nabla\mathcal{H}\rangle)_{xx \text{ or } yy} < 0.$$

The uncertain sign of $\nabla\nabla\mathcal{H}$ explains the presence of wild fluctuations, and even negative configurational temperatures, in the vicinity of the shock front (see Fig. 6). This outlandish behavior means that the configurational temperature is not a useful concept for such problems.

Defining the kinetic temperature requires first of all an average velocity, about which the thermal fluctuations can be computed. The velocity average can be a one-dimensional sum over particles $\{i\}$ sufficiently close to the grid point k,

$$u(x_k) \equiv \sum_i w_{ik}^{1D} v_i / \sum_i w_{ik}^{1D} \to T^{1D}.$$

Alternatively a local velocity can be defined at the location of each particle i by using a two-dimensional Lucy's weight function,

$$w^{2D}(r<h) = (5/\pi h^2)[1 - 6(r/h)^2 + 8(r/h)^3 - 3(r/h)^4],$$

$$r < h = 3,$$

$$\to \int_0^h 2\pi r w(r) dr \equiv 1,$$

and summing over nearby particles $\{j\}$,

$$u(x_i) \equiv \sum_j w_{ij}^{2D} v_j / \sum_j w_{ij}^{2D} \to T^{2D}.$$

These latter two-body sums can either both include or both omit the "self"-term with $i=j$. Our numerical results support the intuition that it is best to omit both the self-terms [17]. We compute all three of these x and y temperature sets for the stationary shock-wave profile and plot the results in Figs. 7 and 8.

The data show that in every case T_{xx} exceeds T_{yy} in the leading edge of the shock front. There is a brief time lag between the leading rise of the longitudinal temperature T_{xx} and the consequent rise of the transverse temperature T_{yy}. This is to be expected from the nature of the shock process, which converts momentum in the x direction into heat [26,27]. The Rayleigh line itself (see again Fig. 2) shows the mechanical analog of this anisotropy, with P_{xx} greatly exceeding P_{yy}. Note that the lower pressure in Fig. 2, the Hugoniot pressure, is a set of equilibrium values, $(P_{xx} + P_{yy})/2$. It is noteworthy that the height of the temperature maximum is sensitive to the definition of the local velocity. Evidently a temperature based on the local velocity, near the particle in question, and with a coarser averaging range $h = 3$ gives a smaller gradient and should accordingly provide a much simpler modeling challenge.

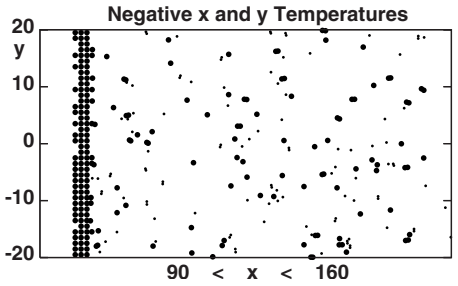

FIG. 6. Particles with *negative* configurational temperatures are shown here, using the data underlying Figs. 4 and 5. The material to the right of the shock is "hot," with cold material entering at the left. The smaller dots correspond to negative values of T_{xx}^Φ and the larger ones correspond to negative T_{yy}^Φ.

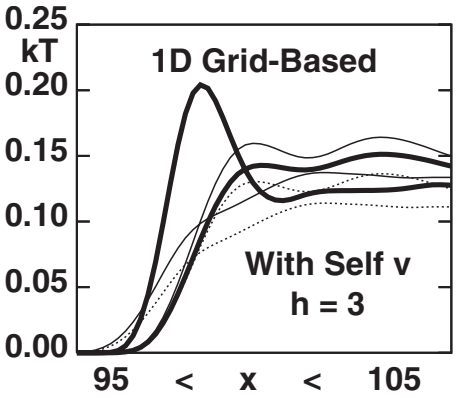

FIG. 7. Typical instantaneous temperature profiles, at $t=5Dt$ for the strong shock wave described in the text. Local particle-based definitions of stream velocity give the two somewhat lower-temperature pairs, (T^K_{xx}, T^K_{yy}). The grid-based definitions of T^K_{xx} and T^K_{yy} are indicated with the heaviest lines. They both use a one-dimensional weight function. This definition gives a strong temperature maximum for T^K_{xx}. In all three cases the longitudinal temperature T^K_{xx} exceeds the transverse temperature T^K_{yy} near the shock front. The temperatures obtained with two-dimensional weights and including the "self"-terms in the average velocity are indicated by the dashed lines and are significantly lower than the rest throughout the hot fluid exiting the shock wave. The "correct" hot temperature, far from the shock, is $kT=0.13$, based on separate equilibrium molecular-dynamics simulations. The profiles shown here were all computed from the instantaneous state of the system after a simulation time of $5Dt=200/u_s$.

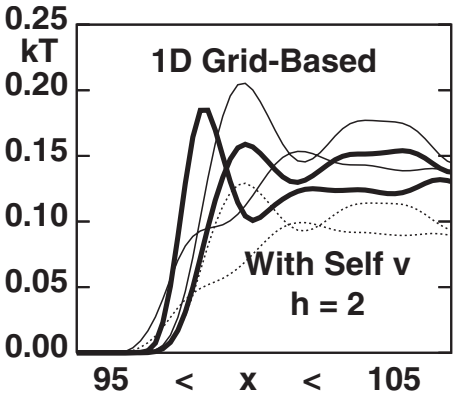

FIG. 8. Temperature profiles with the same data as in Fig. 7, but with a reduced averaging range, $h=2$. Again, the temperatures including "self"-contributions to the local velocity are shown as dashed lines. Notice the sensitivity of the maximum in T^K_{xx} to the range h. Far to the right, the correct hot temperature—at equilibrium, away from the shock—is $kT=0.13$, based on separate equilibrium molecular-dynamics simulations.

IV. SUMMARY

This work shows that planar shock waves are stable for a smooth repulsive potential in a dense fluid. We also find that a mechanical instability makes the configurational temperature quite useless for such problems. Our investigation of temperature definitions shows that relatively smooth instantaneous temperature profiles can be based on the weight functions used in smooth particle applied mechanics. It is noteworthy that the constitutive relations describing inhomogeneous nonequilibrium systems must necessarily include an averaging recipe for the constitutive properties. The present work supports the idea [11] that the range of smooth averages should be at least a few particle diameters.

The better behavior of a particle-based temperature when the "self"-terms are left out is not magic. Consider the equilibrium case of a motionless fluid at the kinetic temperature T. The temperature of a particle in such a system should be measured in a motionless frame. If the "self"-velocity is included in determining the frame velocity, an unnecessary error will occur. Thus it is plausible that the "self"-terms should be left out. The data shown in Figs. 7 and 8 support this view.

The instantaneous particle-based velocity average provides a smoother gentler profile which should be simpler to model. By using an elliptical weight function, much wider in the y direction than the x direction, one could consider the grid-based temperature as a limiting case. The somewhat smoother behavior of the particle-based temperature recommends against taking this limit. The elliptical weight function would leave the divergent configurational temperature unchanged.

ACKNOWLEDGMENTS

We thank Brad Lee Holian for insightful comments on an early version of the manuscript. The comments made by the two referees were helpful in clarifying the temperature concept and its relation to earlier work. Robert J. Hardy was particularly forthcoming and generous in discussing the early history of his approach to making "continuum predictions from molecular-dynamics simulations." We are currently in the process of comparing Hardy's approach to stress with the simpler Lucy approach. The differences are very small. This work was partially supported by the British Engineering and Physical Sciences Research Council and was presented at Warwick in the spring of 2009.

[1] G. E. Duvall and R. A. Graham, Rev. Mod. Phys. **49**, 523 (1977).

[2] L. D. Landau and E. M. Lifshitz, *Fluid Mechanics* (Reed, Oxford, 2000).

[3] G. I. Kanel, W. F. Razorenov, and V. E. Fortov, *Shockwave Phenomena and the Properties of Condensed Matter* (Springer, Berlin, 2004).

[4] W. Nellis, e-print arXiv:0906.0106.

[5] R. E. Duff, W. H. Gust, E. B. Royce, M. Ross, A. C. Mitchell, R. N. Keeler, and W. G. Hoover, *Behavior of Dense Media under High Dynamics Pressures*, Proceedings of the 1967 Paris Conference (Gordon and Breach, New York, 1968).

[6] V. Y. Klimenko and A. N. Dremin, in *Detonatsiya, Chernogolovka*, edited by G. N. Breusov *et al.* (Akad. Nauk, Moscow, 1978), p. 79.
[7] W. G. Hoover, Phys. Rev. Lett. **42**, 1531 (1979).
[8] B. L. Holian, W. G. Hoover, B. Moran, and G. K. Straub, Phys. Rev. A **22**, 2798 (1980).
[9] R. J. Hardy, J. Chem. Phys. **76**, 622 (1982); (private communication); Philippe Choquard (private communication).
[10] O. Kum, Wm. G. Hoover, and C. G. Hoover, Phys. Rev. E **56**, 462 (1997).
[11] S. Root, R. J. Hardy, and D. R. Swanson, J. Chem. Phys. **118**, 3161 (2003).
[12] C. E. Ragan III, Phys. Rev. A **21**, 458 (1980).
[13] H. M. Mott-Smith, Phys. Rev. **82**, 885 (1951).
[14] O. G. Jepps, Ph.D. thesis, Australian National University, Canberra, 2001.
[15] C. Braga and K. P. Travis, J. Chem. Phys. **123**, 134101 (2005).
[16] Wm. G. Hoover and C. G. Hoover, Phys. Rev. E **77**, 041104 (2008).
[17] Wm. G. Hoover and C. G. Hoover, Phys. Rev. E **79**, 046705 (2009).
[18] B. D. Butler, G. Ayton, O. G. Jepps, and D. J. Evans, J. Chem. Phys. **109**, 6519 (1998).
[19] Wm. G. Hoover, C. G. Hoover, and J. F. Lutsko, Phys. Rev. E **79**, 036709 (2009).
[20] L. B. Lucy, Astron. J. **82**, 1013 (1977).
[21] Wm. G. Hoover, *Smooth Particle Applied Mechanics—The State of the Art* (World Scientific Publishers, Singapore, 2006); http://www.worldscibooks.com/mathematics/6218.html
[22] Wm. G. Hoover, *Computational Statistical Mechanics* (Elsevier, Amsterdam, 1991); http://williamhoover.info/book.pdf
[23] W. G. Hoover, B. L. Holian, and H. A. Posch, Phys. Rev. E **48**, 3196 (1993).
[24] W. Hoover, C. Hoover, and M. N. Bannerman, J. Stat. Phys. (to be published).
[25] L. D. Landau and E. M. Lifshitz, *Statistical Physics* (Muir, Moscow, 1951) (in Russian), Eq. 33.14.
[26] B. L. Holian, C. W. Patterson, M. Mareschal, and E. Salomons, Phys. Rev. E **47**, R24 (1993).
[27] B. L. Holian, Phys. Rev. A **37**, 2562 (1988).